

# Robust Mølmer-Sørenson gate for neutral atoms using rapid adiabatic Rydberg dressing

Anupam Mitra,<sup>1,2</sup> Michael J. Martin,<sup>3,4</sup> Grant W. Biedermann,<sup>1,4,5</sup>  
 Alberto M. Marino,<sup>5,4</sup> Pablo M. Poggi,<sup>1,2</sup> and Ivan H. Deutsch<sup>1,2</sup>

<sup>1</sup>*Center for Quantum Information and Control, University of New Mexico, Albuquerque, NM, USA*

<sup>2</sup>*Department of Physics and Astronomy, University of New Mexico, Albuquerque, NM, USA*

<sup>3</sup>*Los Alamos National Laboratory, Los Alamos, NM, USA*

<sup>4</sup>*Sandia National Laboratories, Albuquerque, NM, USA*

<sup>5</sup>*Department of Physics and Astronomy, University of Oklahoma, Norman, OK, USA*

(Dated: 2022-07-19 21:39:28Z)

The Rydberg blockade mechanism is now routinely considered for entangling qubits encoded in ground states of neutral atoms. Challenges towards implementing entangling gates with high fidelity include errors due to thermal motion of atoms, laser amplitude inhomogeneities, imperfect Rydberg blockade, and finite Rydberg state lifetime. We show that adiabatic rapid passage by Rydberg dressing provides a mechanism for implementing two-qubit entangling gates by accumulating phases that are robust to imperfections such as random atomic motion, laser inhomogeneities, and which can accommodate an imperfect blockade. We find that the typical error in implementing a two-qubit gate, such as the controlled phase gate, is dominated by errors in the single atom light shift, and that this can be easily corrected using adiabatic dressing interleaved with a simple spin echo sequence. This results in a two-qubit Mølmer-Sørenson gate. A gate fidelity  $\sim 0.995$  is achievable with modest experimental parameters and a path to higher fidelities is possible for Rydberg states in atoms with a stronger blockade, longer lifetimes, and larger Rabi frequencies.

Arrays of trapped neutral atoms interacting via electric dipole-dipole interactions (EDDI) have emerged as a potential scalable platform for quantum information processing [1–14]. Applications under exploration include quantum simulation of many-body physics [15–26], high precision sensors and metrology [27–32], optimization encoded in Ising graphs [18, 21, 33, 34], and other potential accessible noisy intermediate-scale quantum (NISQ) algorithms [33, 35, 36]. In the longer term, this system is a promising platform for universal fault-tolerant quantum computing given long-lived qubits at the heart of ultraprecise atomic clocks both in the microwave with alkali atoms [37–39] and optical regime with alkaline earths [28, 32, 34, 40], flexible trapping geometries in 1D [41], 2D [42], and 3D [43, 44], and new innovations to create and load defect-free trap arrays [41–44]. Recent experiments in the Weiss group have demonstrated high fidelity, on demand single qubit gates [45, 46] but the implementation of high-fidelity two qubit gates, with long-lived clock qubits in such systems remains a critical challenge [9–14].

The original proposal for implementing entangling quantum logic gates based on EDDI dates back 20 years, whereby hyperfine qubits would receive state-dependent entangling light shifts [1, 2]. This proposal, based on short-lived optically excited dipoles was limited however, as a strong EDDI would require small separation between atoms, which were simultaneously highly localized. By exciting atoms to a high-lying Rydberg state with principal quantum number  $n \geq 50$ , giant long-range EDDI allow for fast entangling gates for separated and addressable atoms on time scale short comparable to the excited state lifetime, as described in the seminal proposal of Jaksch *et al.* [47]. Moreover, the strong EDDI of Rydberg

states enables the dipole-blockade mechanism [3, 9–11] with unique properties for entangling interactions. Seminal experiments by the groups of Browaeys/Grangier [5] and Saffman/Walker [6] showed the first demonstration of such entangling two-qubit interactions. In recent developments, the Lukin group has demonstrated  $> 97\%$  fidelity for creating entangling interactions for qubits encoded in ground and Rydberg states [12] and has applied this in a variety of applications [20, 22, 23]. Moreover, the Lukin group [13] and the Saffman group [14] have recently demonstrated Controlled-Z (CZ) on clock state qubits with fidelity  $> 0.90$ .

A general unitary gate acting on two qubits, such as CZ, has a separable component that acts on each qubit locally and a nonlocal entangling component. As we will see, for the class of unitary gates implemented using EDDI, the gate errors come primarily from the local, separable component. A Mølmer-Sørenson (MS) gate, by contrast, involves only a nonseparable entangling Hamiltonian [48, 49]. We show that implementing the MS gate is the most robust against experimental imperfections and that it can be done using adiabatic Rydberg dressing and a simple spin echo.

Rydberg dressing has been studied in a variety of contexts including many-body physics [15, 16, 19], metrology [30, 32], and quantum simulation [33, 50, 51, 51, 52]. We have employed strong Rydberg dressing to create two-qubit entangled states based on a spin-flip blockade, [8] and measured the light-shifts of the adiabatically dressed entangled states using Autler-Townes spectroscopy [53].

To achieve high fidelity gates, we consider adiabatic rapid passage as a powerful method for implementing robust control [54–57]. In the context of Rydberg EDDI based gates, adiabatic evolution of excited dark states

has been considered as a means of creating gates where the blockade is not strong and to avoid errors due to imperfect blockade and excitation of double Rydberg states [22, 47, 58]. In past work we showed how adiabatic dressing can be employed to implement a CZ gate with the potential for Doppler-free excitation [58]. In the current work we extend our analysis and emphasize how adiabatic Rydberg dressing facilitates the implementation of a MS gate for entangling two qubits with intrinsic robustness to a wide variety of imperfections. These include inhomogeneities in intensity and in detuning, such as those arising from Doppler shifts at finite temperature and Stark shifts from stray electric fields. As we will show, the dominant effect of such inhomogeneities can be removed using a simple spin echo. Moreover, for adiabatic rapid passage, the integrated time spent in the Rydberg state is less than that for the standard pulsed protocol of Jaksch *et al.* with equivalent Rabi frequencies [47], thereby reducing errors due to finite Rydberg radiative lifetime. Gate fidelities  $\sim 99.5\%$  are compatible with the typical inhomogeneities in current experiments and Rydberg state lifetimes  $t \sim 100\mu\text{s}$ . With longer-lived Rydberg states, possible at cryogenic temperatures, optimal control with numerical design can be used to push fidelities greater than 99.99%.

For generality, we consider an atom with two long-lived “clock states” to serve as the qubit states  $|0\rangle$  and  $|1\rangle$ . These could be the hyperfine clock states of alkali atoms separated by a microwave frequency (e.g., Cs or Rb), or the optical clock states of two valence electron atoms (e.g., Sr or Yb). The upper clock  $|1\rangle$  is optically coupled to a high-lying Rydberg state  $|r\rangle$ . As an example we consider  $^{133}\text{Cs}$  as used in our experiment, with qubit states  $|1\rangle = |6\text{S}_{1/2}, F = 4, m_F = 0\rangle$  and  $|0\rangle = |6\text{S}_{1/2}, F = 3, m_F = 0\rangle$  [8, 52, 53, 58], with  $|1\rangle$  coupled through a one-photon transition at 319nm (the “Rydberg laser”) the state  $|r\rangle = |64\text{P}_{3/2}, m_J = 3/2\rangle$ . The qubit states can be connected with microwave or Raman laser fields.

The fundamental Hamiltonian governing the Rydberg gate between two qubits is  $\hat{H}_{\text{2atom}} = \hat{H}_a + \hat{H}_b + V_{\text{DD}}|rr\rangle\langle rr|$  where  $V_{\text{DD}}$  is the electric dipole interaction.  $\hat{H}_a$  ( $\hat{H}_b$ ) is the Hamiltonian for the atom  $a$  ( $b$ ) coupled to the Rydberg laser,

$$\hat{H}_a = \frac{\hat{p}_a^2}{2m} - \Delta_{1r}|r\rangle_a\langle r|_a + \frac{\Omega_{1r}}{2} (e^{ik_r\hat{z}_i}|r\rangle_a\langle 1|_a + \text{h.c.}), \quad (1)$$

where  $\Omega_{1r}$  and  $\Delta_{1r}$  are the Rydberg laser Rabi frequency and detuning respectively (here and throughout we set  $\hbar = 1$ ),  $\hat{p}_a$  is the atomic momentum operator and  $\hat{z}_a$  is the atomic position operator in the direction of the Rydberg laser. We consider the strong blockade regime  $V_{\text{DD}} \gg \Omega_{1r}$  and neglect to zeroth order any population in the doubly excited Rydberg state  $|rr\rangle$ ; corrections will be considered below. Note, we consider here Rydberg interactions for atoms released from a trap, as is typically done in experiments [5, 6, 8, 12–14, 59–61] and treat the

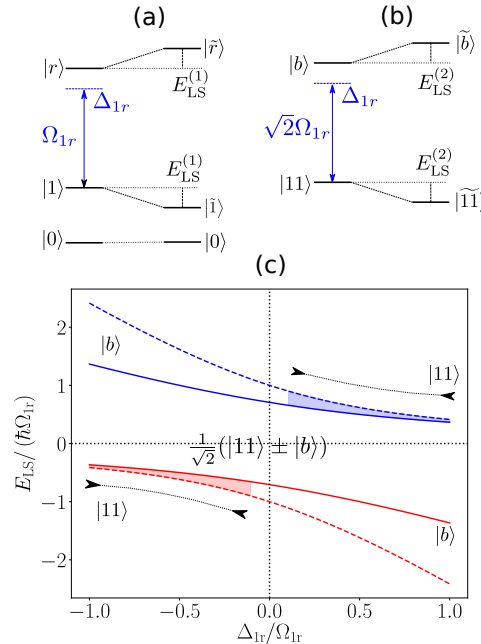


FIG. 1: (a) Qubit encoded into atomic clock states with the upper clock state,  $|1\rangle$ , coupled to a Rydberg state  $|r\rangle$  with a Rabi frequency  $\Omega_{1r}$  and detuning  $\Delta_{1r}$ . (b) The two-atom state  $|11\rangle$  is coupled to the entangled bright state  $|b\rangle$  with Rabi frequency  $\sqrt{2}\Omega_{1r}$ . (c) Light shift of the state  $|11\rangle$  as a function detuning. The dashed lines show the light shift in the absence of EDDI (top: starting from blue detuning, bottom: starting from red detuning), in an adiabatic passage to the doubly excited Rydberg state  $|rr\rangle$ . The solid lines show the light shift in the presence of EDDI under the perfect blockade approximation (top: starting from blue detuning, bottom: starting from red detuning). The shaded region shows the value of  $\kappa$  (Eq. (5)). The dotted lines with arrows show the adiabatic passages used in our ramps to obtain entanglement in the ground state.

motion as that of a free particle.

In the standard protocol of Jaksch *et al.* [47], a series of pulses is applied to the control( $c$ ) and target( $t$ ) qubits,  $\pi_c - 2\pi_t - \pi_c$ , ideally yielding a CZ gate. In the presence of finite thermal atomic velocity, e.g.,  $v_c$  for the control atom, the transformation on the logical states is  $|00\rangle \rightarrow |00\rangle$ ,  $|01\rangle \rightarrow -|01\rangle$ ,  $|10\rangle \rightarrow -e^{-ik_{1r}v_c\delta t}|10\rangle$ ,  $|11\rangle \rightarrow -e^{-ik_{1r}v_c\delta t}|11\rangle$ . Relative to the ideal CZ gate, there are additional phases due to the random Doppler shift acquired when the control atom stays in the Rydberg state for a time  $\delta t$ . For a thermal distribution of momenta, the random distribution of phases cannot be compensated, and is one major contributor to gate infidelity [5, 12–14, 58].

We consider an alternative protocol based on adiabatic Rydberg dressing. We begin with the case of “frozen” atoms at zero velocity. In the ideal protocol, the atoms are illuminated uniformly and see the same Rydberg laser intensity and detuning. Under those conditions it is natural to consider the basis of “bright”

$|b\rangle = (e^{ik_1rz_b}|1, r\rangle + e^{ik_1rz_a}|r, 1\rangle)/\sqrt{2}$  and “dark”  $|d\rangle = (e^{ik_1rz_b}|1, r\rangle - e^{ik_1rz_a}|r, 1\rangle)/\sqrt{2}$  states. Assuming a perfect blockade and atoms with zero momentum, the Rydberg Hamiltonian takes the simple form [16, 58]

$$\hat{H}_{\text{2atom}}(p_a = 0, p_b = 0) = -\Delta_{1r}(|b\rangle\langle b| + |d\rangle\langle d|) + \frac{\sqrt{2}\Omega_{1r}}{2}(|b\rangle\langle 11| + \text{h.c.}). \quad (2)$$

A  $\pi$ -rotation on the  $|11\rangle \rightarrow |b\rangle$  transition yields an entangled state, recently achieved with fidelity 97% [12]. Note, when there is thermal motion, the relative phase  $e^{ik_1r(z_b-z_a)}$  will vary, leading to coupling between bright and dark states, which limits the transfer the entanglement from the bright state to the long-lived ground state qubits [5, 14].

The dressed states of this two-atom Hamiltonian are [62]

$$|\widetilde{11}\rangle = \cos \frac{\theta}{2} |11\rangle + \sin \frac{\theta}{2} |b\rangle \quad (3)$$

$$|\widetilde{b}\rangle = \cos \frac{\theta}{2} |b\rangle - \sin \frac{\theta}{2} |11\rangle, \quad (4)$$

where  $\tan \theta = \sqrt{2}\Omega_{1r}/\Delta_{1r}$ . In the dressed states, some character of the entangled bright state  $|b\rangle$  is admixed with the ground state  $|11\rangle$ . The two-atom light-shift of the ground state, mediated by the Rydberg blockade, is a shift in the eigenvalue of the dressed states with respect to the bare states, which under the perfect blockade approximation is  $E_{\text{LS}}^{(2)} = \frac{1}{2}(-\Delta_{1r} \pm \sqrt{2\Omega_{1r}^2 + \Delta_{1r}^2})$  [16, 47, 58]. The difference between this light shift,  $E_{\text{LS}}^{(1)}$ , and twice that of the single atom light shift with no EDDI is the *entangling energy scale*,  $\kappa$  [8, 53, 58]

$$\begin{aligned} \kappa &= E_{\text{LS}}^{(2)} - 2E_{\text{LS}}^{(1)} \\ &= \frac{\Delta_{1r}}{2} \pm \frac{1}{2} \left( \sqrt{2\Omega_{1r}^2 + \Delta_{1r}^2} - 2\sqrt{\Omega_{1r}^2 + \Delta_{1r}^2} \right). \end{aligned} \quad (5)$$

On resonance  $\kappa \approx \pm 0.29\Omega_{1r}$ , where  $\Omega$  can be as large as a few MHz [53]. For weak dressing,  $|\Delta_{1r}| \gg \Omega_{1r}$ ,  $\kappa \approx -\Omega_{1r}^4/8\Delta_{1r}^3$ , which will generally smaller than the rate of photon scattering, which scales as  $1/\Delta_{1r}^2$  [53, 58]. Thus weak dressing will not yield high fidelity entangling gates in our protocol.

The dressed energy levels provide an adiabatic passage from the one-atom ground state  $|1\rangle$  to the one-atom Rydberg state  $|r\rangle$  and from the two-atom ground state  $|11\rangle$  to the two-atom entangled bright state  $|b\rangle$ , as shown in Fig. 1. Assuming adiabatic evolution, we restrict our consideration to sweeping the detuning from  $|11\rangle$  toward  $|b\rangle$  and then back to  $|11\rangle$ , yielding an entangling phase given by  $\vartheta_2 = \int \kappa dt$ . While  $\kappa$  grows monotonically as we pass adiabatically from  $|11\rangle$  to  $|b\rangle$ , the simultaneous restrictions of adiabaticity and limiting the phase  $\vartheta_2$  to the target value restricts the value of the final detuning. Operationally this final detuning is near resonance in our

protocol, yielding the minimum gate time such that we simultaneously remain adiabatic but act fast compared to the decoherence rates.

To understand the general class of gates enabled by the phases accumulated in adiabatic evolution and their sensitivity to errors, we consider the Hamiltonian in the dressed qubit (DQ) ground subspace  $\{|00\rangle, |01\rangle, |\widetilde{10}\rangle, |\widetilde{11}\rangle\}$ . Let  $\hat{\sigma}_z = |\widetilde{1}\rangle\langle\widetilde{1}| - |0\rangle\langle 0|$  be the adiabatic Pauli operator on one atom and  $\hat{S}_z = \mathbb{1} \otimes \hat{\sigma}_z/2 + \hat{\sigma}_z/2 \otimes \mathbb{1}$  be the collective angular momentum operator. In the dressed atomic basis, the Hamiltonian in the ground subspace is [63]

$$\hat{H}_{\text{DQ}} = -\left(E_{\text{LS}}^{(1)} + \frac{\kappa}{2}\right)\hat{S}_z + \kappa \frac{\hat{S}_z^2}{2} \quad (6)$$

This Hamiltonian generates symmetric, one axis, two qubit unitary transformations. The  $\hat{S}_z$  term generates  $\text{SU}(2)$  rotations on the collective spin, while the  $\hat{S}_z^2$  term “twists” the collective spin and also generates two-qubit entanglement. The quantization axis can be changed to any axis  $\mu$  using additional global  $\text{SU}(2)$  rotations. Consider, thus, the unitary transformation of the dressed qubits generated by adiabatic evolution with this Hamiltonian,

$$\hat{U}_\kappa = \exp \left( -i\vartheta_1 \hat{S}_\mu - i\vartheta_2 \frac{\hat{S}_\mu^2}{2} \right), \quad (7)$$

where  $\vartheta_1 = -\int \left(E_{\text{LS}}^{(1)} + \frac{\kappa}{2}\right) dt$  is the rotation angle generated by the linear term, and  $\vartheta_2 = \int \kappa dt$  is the twist angle generated by the quadratic term in the Hamiltonian.

When the twist angle  $\vartheta_2 = \pm\pi$ , these gates are perfect entanglers [64], meaning that the gates can take a product state to a maximally entangled state. Examples of perfect entanglers of this kind are the CZ gate ( $\mu = z, \vartheta_1 = \mp\pi/2, \vartheta_2 = \pm\pi$ ) and the MS gate ( $\mu = x, \vartheta_1 = 0, \vartheta_2 = \pi$ ). A CZ gate is achieved by removing the phases accumulated due to the independent one atom light shifts  $E_{\text{LS}}^{(1)}$  [58]. In contrast, the MS gate is achieved by removing *all* single qubit phases contributing to  $\vartheta_1$ . Formally, the Lie algebra generating the group of two-qubit gates,  $\mathfrak{su}(4)$ , has a Cartan decomposition  $\mathfrak{su}(4) = \mathfrak{p} \oplus \mathfrak{k}$  where  $\mathfrak{p}$  is the algebra generated by all one qubit Pauli operators (linear powers of collective spin operators), that is the generators of  $\text{SU}(2) \otimes \text{SU}(2)$  and  $\mathfrak{k}$  is the algebra generated by all two qubit Pauli operators (quadratic powers of collective spin operators) [64–66]. The entanglement between qubits is generated by the subalgebra  $\mathfrak{k}$  and we can remove terms arising from subalgebra  $\mathfrak{p}$  with no affect on the universal gate set. While theoretically this difference is trivial, in practice, this has critical importance in the sensitivity to errors.

To implement a two-qubit gate of the form Eq. (7) we consider an adiabatic ramp involving sweeping both the laser amplitude, proportional to  $\Omega_{1r}$ , and the frequency,

related to  $\Delta_{1r}$ , to dress ground states with Rydberg character and undress them. This implements a rapid adiabatic passage from each atom's  $|1\rangle$  state to a near equal superposition of  $|1\rangle$  and  $|r\rangle$ , staying in this superposition and a rapid adiabatic passage back to  $|1\rangle$ . Moreover, it simultaneously implements a rapid adiabatic passage from the two atom state  $|11\rangle$  to a near equal superposition of  $|11\rangle$  and the bright state  $|b\rangle$ , staying in this superposition and a rapid adiabatic passage back to  $|11\rangle$ . In particular, we design the dressing ramp through half Gaussian ramp of  $\Omega_{1r}$  from  $\Omega_{\min}$  to the maximum Rabi frequency,  $\Omega_{\max}$  and a linear ramp of the detuning  $\Delta_{1r}$  towards resonance, from time  $t_1$  to  $t_2$  as

$$|\Delta_{1r}(t)| = \Delta_{\max} + \frac{(\Delta_{\max} - \Delta_{\min})}{(t_2 - t_1)}(t - t_1) \quad (8)$$

$$\Omega_{1r}(t) = \Omega_{\min} + (\Omega_{\max} - \Omega_{\min}) \exp\left(-\frac{(t - t_2)^2}{2t_w^2}\right)$$

followed by staying constant from time  $t_2$  to  $t_3$  and finally undressing from  $t_3$  to  $t_4$  by reversing the dressing ramp. The parameters of the ramp are optimized to achieve a particular value of  $\vartheta_2$ . To implement the MS gate, we consider two adiabatic ramps, each achieving an entangling phase of  $\vartheta_2 = \pm\pi/2$ , with an echo pulse on the qubit transition,  $\exp(-i\pi\hat{S}_x)$  between them as done in [63]. The echo pulse cancels the  $\vartheta_1$  accumulated in the two adiabatic ramps, thus implementing a MS gate about the  $z$  axis. We convert this to a MS gate about the  $y$  axis using  $\pi/2$  rotations about the  $x$  axis. An advantage of using these adiabatic ramps is they can be designed to for any value of  $\vartheta_2$ , not just integer multiples for  $\pi$  as in the  $\pi_c - 2\pi_t - \pi_c$  sequence. The duration of this ramp, implementing  $\vartheta_2 = \pi/2$ , shown in Fig. 2 is  $\approx 8.4 \times 2\pi/\Omega_{\max}$ . We find the time spent in Rydberg states as the time integrated Rydberg population,  $t_r = \int dt' \mathcal{P}_r(t')$  to be  $0.7 \times 2\pi/\Omega_{\max}$  for initial states  $|01\rangle$  and  $|10\rangle$  and  $0.9 \times 2\pi/\Omega_{\max}$  for initial state  $|11\rangle$ . As long as the Rabi period  $2\pi/\Omega_{\max}$  is much larger than the radiative life time of the Rydberg states, these ramps are rapid and have small loss due to Rydberg state decay. Starting in  $|11\rangle$  leads to time spent in the doubly excited Rydberg state  $|rr\rangle$  of  $0.0029 \times 2\pi/\Omega_{\max}$  when the EDDI is a modest, e.g.,  $V_{DD} = 10\Omega_{\max}$  for  $\Omega_{\max}$  of a few MHz. The population dynamics, during the ramp are shown in Fig. 2.

We assess the performance of the gate by considering the fidelity between the implemented two-qubit gate,  $\hat{U}$ , and the target ideal unitary transformation  $\hat{V}$  defined using a normalized Hilbert Schmidt inner product between them  $\mathcal{F} = |\text{tr}(\hat{U}\hat{V}^\dagger)|^2/16$  [67]. In particular, consider errors that can arise from inhomogeneities or coherent errors in the accumulated phases. The fidelity depends on the difference between twist angles  $\delta\vartheta_2$  and the difference between rotation angles  $\delta\vartheta_1$  of the implemented

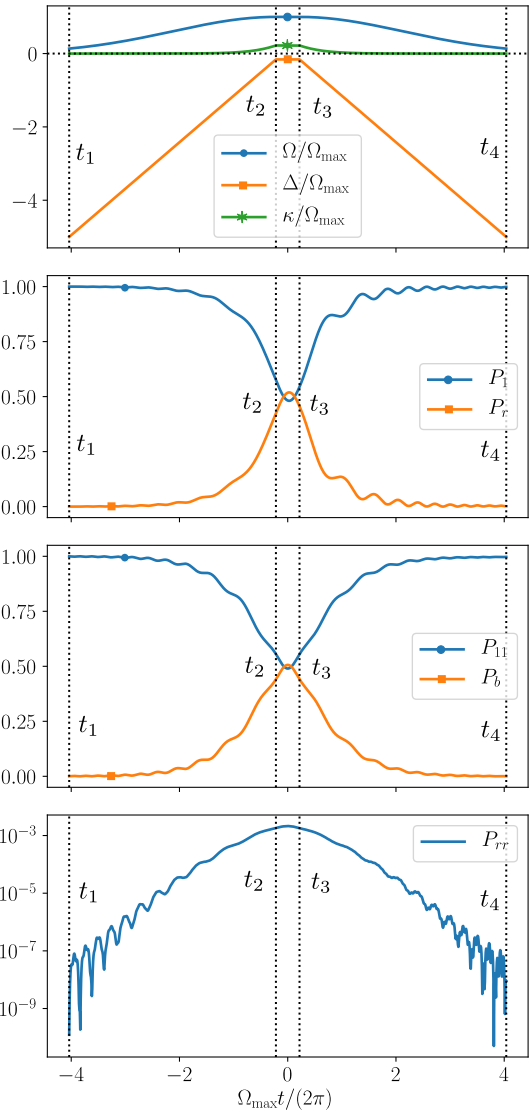


FIG. 2: Adiabatic ramp to implement a unitary transformation in Eq. (7) with  $\vartheta_2 = \pi/2$ . First panel: blue line (circle) shows the Rabi frequency, orange line (square) shows the detuning and the green line (star) shows the entangling energy as a function of time during the ramp. Second panel: blue line (circle) shows the population of  $|01\rangle$  and  $|10\rangle$  and orange line (square) shows the population of  $|0r\rangle$  and  $|r0\rangle$ . Third panel: blue line (circle) shows the population of  $|11\rangle$  and orange line (square) shows the population of  $|b\rangle$ . Fourth panel: population of  $|rr\rangle$  in a logarithmic scale.

and target unitary maps according to

$$\mathcal{F} = \frac{1}{4} \left( 1 + \cos^2(\delta\vartheta_1) + 2 \cos(\delta\vartheta_1) \cos\left(\frac{\delta\vartheta_2}{2}\right) \right). \quad (9)$$

Importantly, the fidelity is much more sensitive to  $\delta\vartheta_1$  than it is to  $\delta\vartheta_2$ . The twist angle  $\vartheta_2$  depends solely on the entangling energy  $\kappa$ . As this is the *difference* of two light shifts, it has some common mode cancellation

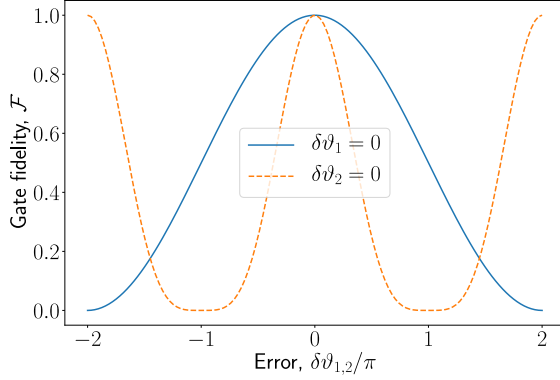


FIG. 3: Fidelity between two one axis twist and rotate unitary transformations (Eq. (7)) as a function of error in the rotation angle  $\delta\vartheta_1$  (blue, solid line) and as function of error in the twist angle  $\delta\vartheta_2$  (orange, dotted line). The fidelity is much more sensitive to  $\delta\vartheta_1$ , which can be made to vanish using a spin echo.

of errors in the light shifts, while  $\vartheta_1$  has a contribution from independent single-atom light shifts with no such cancellation. This effect is seen in Fig. 3 which shows the fidelity plotted as a function of  $\delta\vartheta_1$  when  $\delta\vartheta_2 = 0$  and as a function of  $\delta\vartheta_2$  when  $\delta\vartheta_1 = 0$ . Note, the CZ gate studied in [58] required knowledge of  $E_{\text{LS}}^{(1)}$  to remove the single-

atom contribution to the phase, and errors will contribute substantially to infidelity through  $\delta\vartheta_1$ . In contrast, the MS gate is substantially less sensitive to such errors, as  $\delta\vartheta_1$  can be made zero by using a spin echo as done in [63].

Let us consider the error channels and the intrinsic robustness of using adiabatic Rydberg dressing to implement the MS gate. Deleterious effects include thermal Doppler shifts and atomic motion in a spatially inhomogeneous exciting laser [8, 9, 11, 14, 58, 60], imperfect blockade [8, 9, 33, 58], and finite radiative lifetime of the Rydberg state [9, 11–14, 60]. High-fidelity gates are possible at room temperature with modest radiative lifetimes, consistent with the demands of adiabatic evolution. To see how this effect arises, let us revisit the dressed states, including the quantized motion. For generality we include quantized atomic momenta  $p_a$  and  $p_b$  of the two atoms in their Rydberg dressing interaction in addition to the electronic ground state and the bright and dark states. The bare states are

$$|G\rangle = |1, p_a; 1, p_b\rangle$$

$$|B\rangle = \frac{1}{\sqrt{2}} (|r, p_a + k_{1r}; 1, p_b\rangle + |1, p_a; r, p_b + k_{1r}\rangle) \quad (10)$$

$$|D\rangle = \frac{1}{\sqrt{2}} (|r, p_a + k_{1r}; 1, p_b\rangle - |1, p_a; r, p_b + k_{1r}\rangle).$$

The two-atom Rydberg Hamiltonian now generalizes to [58]

$$\hat{H}_{\text{2atom}}(p_a, p_b) = - \left( \Delta_{1r} - \frac{k_{1r}P_{\text{CM}}}{M} \right) (|B\rangle\langle B| + |D\rangle\langle D|) + \frac{k_{1r}p_{\text{rel}}}{m} (|B\rangle\langle D| + \text{h.c.})$$

$$+ \frac{1}{2} \left( \frac{\Omega_a + \Omega_b}{\sqrt{2}} \right) (|B\rangle\langle G| + |rr\rangle\langle B| + \text{h.c.}) + \frac{1}{2} \left( \frac{\Omega_a - \Omega_b}{\sqrt{2}} \right) (|D\rangle\langle G| + |rr\rangle\langle D| + \text{h.c.})$$

$$+ \left( V_{\text{DD}} - 2 \left( \Delta_{1r} - \frac{k_{1r}P_{\text{CM}}}{M} \right) \right) |rr\rangle\langle rr| \quad (11)$$

where  $\Omega_a = \Omega_{1r}(z_a)$  and  $\Omega_b = \Omega_{1r}(z_b)$  are the Rabi frequencies at the positions of atoms  $a$  and  $b$ ;  $P_{\text{CM}} = p_a + p_b$  and  $p_{\text{rel}} = (p_a - p_b)/2$  are the center-of-mass and relative momenta of the atoms [58]. We have not included here the kinetic energy term common to all states as it leads to no relative phase, and the recoil shift is absorbed into the definition of the detuning.

The effect of the Doppler shift on the dressing gate is now apparent. In contrast to the direct excitation to Rydberg states, as in the standard  $\pi_c - 2\pi_t - \pi_c$  pulse protocol [47], there are no random phases imparted to the qubits as described earlier. Instead, for the dressing protocol, the center-of-mass motion leads to a detuning error [58]. The relative motion leads to coupling between bright and dark states as discussed above. However, while using an adiabatic ramp, this is sup-

pressed due to the energy gap between the light-shifted bright state and unshifted dark state. The residual off-resonance  $|\tilde{B}\rangle \rightarrow |D\rangle$  coupling leads to a small second order perturbative shift on the dressed ground state [58]. Moreover, a nonuniform intensity in which atoms see different Rabi frequencies can introduce a coupling between the ground  $|11\rangle$  and the dark state  $|D\rangle$ , which gives a small perturbative shift on the dressed ground state.

Finally there is the effect of imperfect blockade. Whereas in the standard pulsed protocol this is can be a major source of error, gates based on adiabatic dressing are more resilient to this effect. As long as the evolution is adiabatic, the dressed ground states will contain a small admixture of doubly-excited Rydberg states in the superposition as shown in Fig. 2. This will affect the value of  $\kappa$ , but this can be measured, and the adia-

atic ramp can be adjusted accordingly. If we are close to the blockade radius, the dressed ground state energy as a function of separation between the atoms will be small, and there will be negligible force on the atoms due to the EDDI. Of course non-adiabatic effects such as resonant excitation to other doubly-excited Rydberg states can add additional errors, but these effects are not studied here.

As an example, we take the maximum Rydberg Rabi frequency to be  $\Omega_{\max}/2\pi = 4$  MHz on resonance coupling the states  $|1\rangle$  and  $|r\rangle$ , giving an entangling strength of  $\kappa/2\pi \approx 1.17$  MHz under the perfect blockade approximation. A contribution to detuning inhomogeneities arises from the Doppler width of atomic momentum distribution,  $\delta\Delta_{1r} \propto \sqrt{k_B T/m}$  [5, 14, 60, 61, 68]. With these parameters, an atomic temperature of 10  $\mu\text{K}$  [53] corresponds to  $\delta\Delta_{1r}/\Omega_{1r} \approx 0.02$ . The laser amplitude inhomogeneities can arise, e.g., from interatomic axis not being aligned with the direction of laser propagation. If the transverse alignment of the atoms is off the laser propagation direction by 0.01, we have  $\delta\Omega_{1r}/\Omega_{1r} \approx 0.01$ .

To simulate the experimental scenario, we model the small changes to the light shifts due to atomic motion by considering the detuning  $\Delta_{1r}$  and Rabi frequency  $\Omega_{1r}$  for each atom to be sampled from a normal distribution with mean equal to the fiducial value and standard deviation determined by the level of imperfections in the experiment. We simulate the implementation of the CZ gate using the protocol proposed earlier [58] and the implementation of the MS gate using two adiabatic ramps and a spin echo, over a range of inhomogeneities  $\delta\Delta_{1r}$  and  $\delta\Omega_{1r}$ . The gate fidelity including inhomogeneities, imperfect blockade, and Rydberg state decay for an EDDI strength of  $10\Omega_{\max}$  and the target gate is shown in Fig. 4 (a) for the CZ gate Fig. 4 (b) for the MS gate. We see that implementing the MS gate using two adiabatic ramps and a spin echo is much more robust to inhomogeneities in  $\Omega_{1r}$  and  $\Delta_{1r}$  than implementing the CZ gate using an adiabatic (Fig. 4). For example, when we increase the level of imperfections from 0 to about 10% of the maximum Rabi frequency  $\Omega_{\max}$  in the Rabi frequency and detuning, the MS gate fidelity falls from 0.997 about 0.995, while the CZ gate fidelity falls from about 0.997 to about 0.986. The primary sources of error, which are present even for no inhomogeneities, are finite Rydberg lifetime and imperfect adiabaticity of the adiabatic ramp.

Ultimately, the best achievable adiabaticity is limited by the finite radiative lifetime of Rydberg states, which is the fundamental source of error [9, 11]. The effective lifetime  $\tau_r$  is due to contributions of different decay channels including ionization, spontaneous emission, and stimulated emission via coupling to blackbody radiation [9, 11, 58, 60, 61]. To maximize fidelity, the time spent in the Rydberg state needs to be small compared to the radiative lifetime of the Rydberg state. This can be estimated by the quantity  $\pi/(\kappa\tau_r)$  which compares how quickly atoms decay versus how quickly they accumulate entangling phase. The entangling phase is accumulated faster with a larger Rabi frequency,  $\Omega_{1r}$ . More precisely, the time spent by atoms in the Rydberg state is quantified by the integrated Rydberg population, described above. Optimizing the parameters of the adiabatic ramp, we can satisfy  $t_r/\tau_r \ll 1$  as long as  $\Omega_{\max}\tau_r \ll 1$ . For example, a lifetime of  $\tau_r = 140\mu\text{s}$  [12, 69] and a Rabi frequency of  $\Omega_{1r}/2\pi = 4\text{MHz}$  at resonance with  $\kappa/2\pi \approx 1.17\text{MHz}$  corresponds to  $\pi/(\kappa\tau_r) \approx 3 \times 10^{-3}$ . Lifetimes of a few milliseconds can be achieved by choosing higher Rydberg states and cooling the blackbody radiation to a few Kelvin [11] would give  $\pi/(\kappa\tau_r) \sim 10^{-4}$ .

In summary, adiabatic Rydberg dressing provides a robust method for harnessing the EDDI between Rydberg excited atoms to generate entanglement between qubits encoded in atomic clock states. We have shown that with current experimental capabilities, a two qubit MS entangling gate with a fidelity of  $\sim 0.995$  is within reach by interleaving of adiabatic Rydberg dressing and undressing with a spin echo on the qubit transition. Even higher fidelity gates are possible at cryogenic temperatures which substantially increases the Rydberg state lifetime. Such longer coherence times allow for improved adiabatic ramps and the potential use of more sophisticated robust control and dynamical decoupling [66, 70–72] to correct residual inhomogeneities not canceled in simple spin echo.

We thank Christiane Koch and David Weiss for helpful discussions. This work was supported by NSF grants PHY-1606989, PHY-1630114, the Laboratory Directed Research and Development program at Sandia National Laboratories, and by the Laboratory Directed Research and Development program of Los Alamos National Laboratory under project numbers 20190494ER and 20200015ER.

---

[1] Gavin K Brennen, Carlton M Caves, Poul S Jessen, and Ivan H Deutsch. Quantum logic gates in optical lattices. *Physical Review Letters*, 82(5):1060, 1999.

[2] Gavin K Brennen, Ivan H Deutsch, and Poul S Jessen. Entangling dipole-dipole interactions for quantum logic with neutral atoms. *Physical Review A*, 61(6):062309, 2000.

[3] D Jaksch, H-J Briegel, JI Cirac, CW Gardiner, and P Zoller. Entanglement of atoms via cold controlled collisions. *Physical Review Letters*, 82(9):1975, 1999.

[4] Immanuel Bloch. Quantum coherence and entanglement with ultracold atoms in optical lattices. *Nature*, 453(7198):1016, 2008.

[5] Tatjana Wilk, A Gaëtan, C Evellin, J Wolters, Y Miroshnychenko, P Grangier, and A Browaeys. Entanglement of two individual neutral atoms using rydberg blockade. *Physical Review Letters*, 104(1):010502, 2010.

[6] L Isenhower, E Urban, XL Zhang, AT Gill, T Henage,

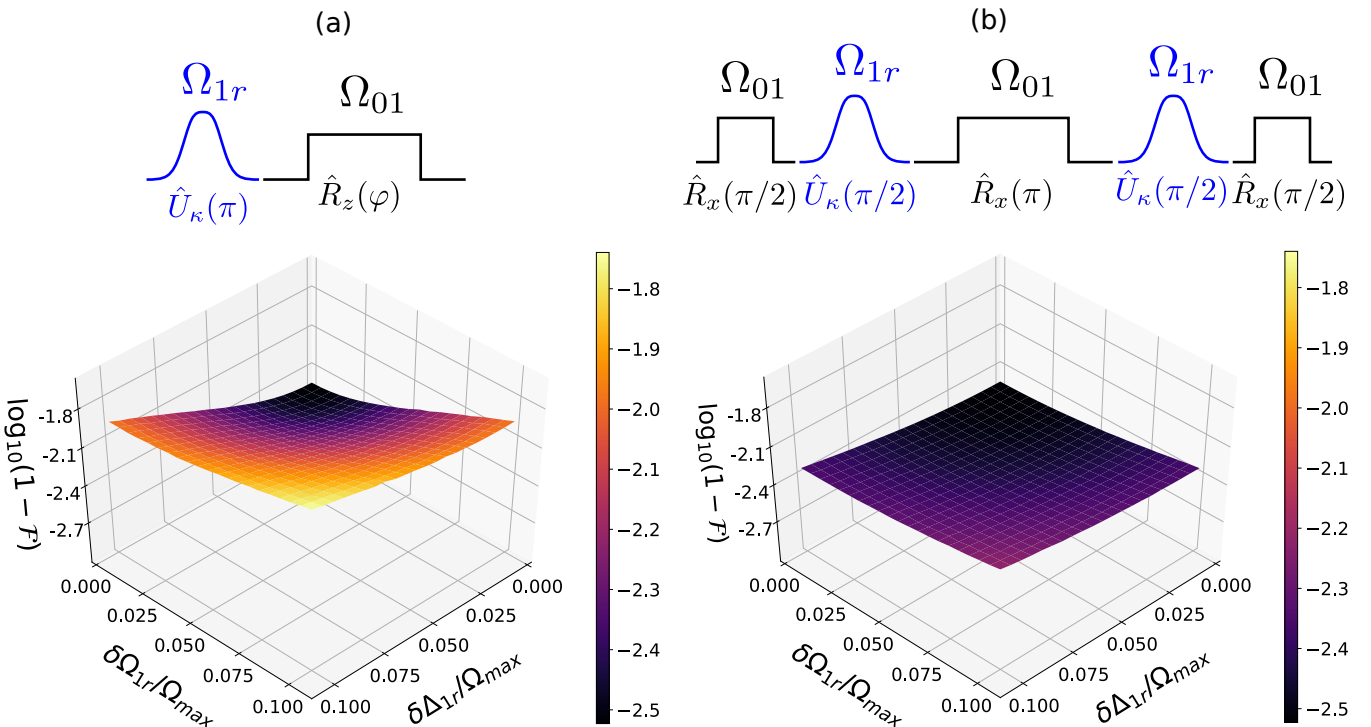


FIG. 4: (a) Top: Implementing the CZ gate as suggested in [58] using an adiabatic ramp, followed by removal of phases accumulated due to one atom light shifts using a single qubit rotation  $\hat{R}_x(\varphi)$ , where  $\varphi = \int dt' E_{\text{LS}}^{(1)}(t')$ . Bottom: Simulated infidelities of implementing the CZ gate with different levels of inhomogeneities in  $\Delta_{1r}$  and  $\Omega_{1r}$ . (b) Top: Implementing the MS gate as done in [63] using two adiabatic ramps, with a spin echo in between. Bottom: Simulated infidelities of implementing the MS gate with different levels of inhomogeneities in  $\Delta_{1r}$  and  $\Omega_{1r}$ .

Todd A Johnson, TG Walker, and M Saffman. Demonstration of a neutral atom controlled-not quantum gate. *Physical Review Letters*, 104(1):010503, 2010.

[7] Jonathan Simon, Waseem S Bakr, Ruichao Ma, M Eric Tai, Philipp M Preiss, and Markus Greiner. Quantum simulation of antiferromagnetic spin chains in an optical lattice. *Nature*, 472(7343):307, 2011.

[8] Y-Y Jau, AM Hankin, T Keating, IH Deutsch, and GW Biedermann. Entangling atomic spins with a rydberg-dressed spin-flip blockade. *Nature Physics*, 12(1):71–74, 2016.

[9] Mark Saffman, Thad G Walker, and Klaus Mølmer. Quantum information with rydberg atoms. *Reviews of Modern Physics*, 82(3):2313, 2010.

[10] David S Weiss and Mark Saffman. Quantum computing with neutral atoms. *Physics Today*, 70(7), 2017.

[11] Mark Saffman. Quantum computing with atomic qubits and rydberg interactions: progress and challenges. *Journal of Physics B: Atomic, Molecular and Optical Physics*, 49(20):202001, 2016.

[12] Harry Levine, Alexander Keesling, Ahmed Omran, Hannes Bernien, Sylvain Schwartz, Alexander S Zibrov, Manuel Endres, Markus Greiner, Vladan Vuletić, and Mikhail D Lukin. High-fidelity control and entanglement of rydberg-atom qubits. *Physical Review Letters*, 121(12):123603, 2018.

[13] Harry Levine, Alexander Keesling, Giulia Semeghini, Ahmed Omran, Tout T Wang, Sepehr Ebadi, Hannes Bernien, Markus Greiner, Vladan Vuletić, Hannes Pichler, et al. Parallel implementation of high-fidelity multi-qubit gates with neutral atoms. *arXiv preprint arXiv:1908.06101*, 2019.

[14] TM Graham, M Kwon, B Grinkemeyer, Z Marra, X Jiang, MT Lichtman, Y Sun, M Ebert, and M Saffman. Rydberg mediated entanglement in a two-dimensional neutral atom qubit array. *arXiv preprint arXiv:1908.06103*, 2019.

[15] Thomas Pohl, Thomas Pattard, and Jan M Rost. Plasma formation from ultracold rydberg gases. *Physical Review A*, 68(1):010703, 2003.

[16] JE Johnson and SL Rolston. Interactions between rydberg-dressed atoms. *Physical Review A*, 82(3):033412, 2010.

[17] YO Dudin and A Kuzmich. Strongly interacting rydberg excitations of a cold atomic gas. *Science*, 336(6083):887–889, 2012.

[18] Henning Labuhn, Daniel Barredo, Sylvain Ravets, Sylvain De Léséleuc, Tommaso Macrì, Thierry Lahaye, and Antoine Browaeys. Tunable two-dimensional arrays of single rydberg atoms for realizing quantum ising models. *Nature*, 534(7609):667, 2016.

[19] Johannes Zeiher, Rick Van Bijnen, Peter Schauß, Sebastian Hild, Jae-yoon Choi, Thomas Pohl, Immanuel Bloch, and Christian Gross. Many-body interferometry of a rydberg-dressed spin lattice. *Nature Physics*, 12(12):1095, 2016.

[20] Hannes Bernien, Sylvain Schwartz, Alexander Keesling, Harry Levine, Ahmed Omran, Hannes Pichler, Soon-

won Choi, Alexander S Zibrov, Manuel Endres, Markus Greiner, et al. Probing many-body dynamics on a 51-atom quantum simulator. *Nature*, 551(7682):579, 2017.

[21] Sylvain De Léséleuc, Sebastian Weber, Vincent Lienhard, Daniel Barredo, Hans Peter Büchler, Thierry Lahaye, and Antoine Browaeys. Accurate mapping of multilevel rydberg atoms on interacting spin-1/2 particles for the quantum simulation of ising models. *Physical review letters*, 120(11):113602, 2018.

[22] Ahmed Omran, Harry Levine, Alexander Keesling, Giulia Semeghini, Tout T Wang, Sepehr Ebadi, Hannes Bernien, Alexander S Zibrov, Hannes Pichler, Soonwon Choi, et al. Generation and manipulation of schrödinger cat states in rydberg atom arrays. *arXiv preprint arXiv:1905.05721*, 2019.

[23] Alexander Keesling, Ahmed Omran, Harry Levine, Hannes Bernien, Hannes Pichler, Soonwon Choi, Rhine Samajdar, Sylvain Schwartz, Pietro Silvi, Subir Sachdev, et al. Quantum kibble–zurek mechanism and critical dynamics on a programmable rydberg simulator. *Nature*, 568(7751):207, 2019.

[24] Alessio Celi, Benoît Vermersch, Oscar Viyuela, Hannes Pichler, Mikhail D Lukin, and Peter Zoller. Emerging 2d gauge theories in rydberg configurable arrays. *arXiv preprint arXiv:1907.03311*, 2019.

[25] Soonwon Choi, Christopher J Turner, Hannes Pichler, Wen Wei Ho, Alexios A Michailidis, Zlatko Papić, Maksym Serbyn, Mikhail D Lukin, and Dmitry A Abanin. Emergent  $su(2)$  dynamics and perfect quantum many-body scars. *Physical Review Letters*, 122(22):220603, 2019.

[26] Joonhee Choi, Hengyun Zhou, Helena S Knowles, Renate Landig, Soonwon Choi, and Mikhail D Lukin. Robust dynamic hamiltonian engineering of many-body spin systems. *arXiv preprint arXiv:1907.03771*, 2019.

[27] Matthew D Swallows, Michael Bishof, Yige Lin, Sebastian Blatt, Michael J Martin, Ana Maria Rey, and Jun Ye. Suppression of collisional shifts in a strongly interacting lattice clock. *science*, 331(6020):1043–1046, 2011.

[28] BJ Bloom, TL Nicholson, JR Williams, SL Campbell, M Bishof, X Zhang, W Zhang, SL Bromley, and J Ye. An optical lattice clock with accuracy and stability at the 10- 18 level. *Nature*, 506(7486):71, 2014.

[29] MJ Martin, M Bishof, MD Swallows, X Zhang, C Benko, J Von-Stecher, AV Gorshkov, AM Rey, and Jun Ye. A quantum many-body spin system in an optical lattice clock. *Science*, 341(6146):632–636, 2013.

[30] LIR Gil, R Mukherjee, EM Bridge, MPA Jones, and T Pohl. Spin squeezing in a rydberg lattice clock. *Physical review letters*, 112(10):103601, 2014.

[31] Hengyun Zhou, Joonhee Choi, Soonwon Choi, Renate Landig, Alexander M Douglas, Junichi Isoya, Fedor Jelezko, Shinobu Onoda, Hitoshi Sumiya, Paola Cappellaro, et al. Quantum metrology with strongly interacting spin systems. *arXiv preprint arXiv:1907.10066*, 2019.

[32] Matthew A Norcia, Aaron W Young, William J Eckner, Eric Oelker, Jun Ye, and Adam M Kaufman. Second-scale coherence on an optical clock transition in a tweezer array. *Science*, page eaay0644, 2019.

[33] Tyler Keating, Krittika Goyal, Yuan-Yu Jau, Grant W Biedermann, Andrew J Landahl, and Ivan H Deutsch. Adiabatic quantum computation with rydberg-dressed atoms. *Physical Review A*, 87(5):052314, 2013.

[34] Ivaylo Madjarov, Jacob Covey, Alexandre Cooper, Adam Shaw, Vladimir Schkolnik, Ryan White, Jason Williams, and Manuel Endres. Strontium atom arrays: toward rydberg entanglement and optical qubit control. *Bulletin of the American Physical Society*, 2019.

[35] Leo Zhou, Sheng-Tao Wang, Soonwon Choi, Hannes Pichler, and Mikhail D Lukin. Quantum approximate optimization algorithm: performance, mechanism, and implementation on near-term devices. *arXiv preprint arXiv:1812.01041*, 2018.

[36] Hannes Pichler, Sheng-Tao Wang, Leo Zhou, Soonwon Choi, and Mikhail D Lukin. Computational complexity of the rydberg blockade in two dimensions. *arXiv preprint arXiv:1809.04954*, 2018.

[37] C Monroe, Hugh Robinson, and C Wieman. Observation of the cesium clock transition using laser-cooled atoms in a vapor cell. *Optics letters*, 16(1):50–52, 1991.

[38] E Tiesinga, BJ Verhaar, HTC Stoof, and D Van Bragt. Spin-exchange frequency shift in a cesium atomic fountain. *Physical Review A*, 45(5):R2671, 1992.

[39] Patrick Joachim Windpassinger, Daniel Oblak, PG Petrov, M Kubasik, M Saffman, CL Garrido Alzar, Jürgen Appel, Jörg Helge Müller, Niels Kjærgaard, and Eugene Simon Polzik. Nondestructive probing of rabi oscillations on the cesium clock transition near the standard quantum limit. *Physical review letters*, 100(10):103601, 2008.

[40] Jacob P Covey, Ivaylo S Madjarov, Alexandre Cooper, and Manuel Endres. 2000-times repeated imaging of strontium atoms in clock-magic tweezer arrays. *Physical review letters*, 122(17):173201, 2019.

[41] Manuel Endres, Hannes Bernien, Alexander Keesling, Harry Levine, Eric R Anschuetz, Alexandre Krajenbrink, Crystal Senko, Vladan Vuletic, Markus Greiner, and Mikhail D Lukin. Atom-by-atom assembly of defect-free one-dimensional cold atom arrays. *Science*, 354(6315):1024–1027, 2016.

[42] Daniel Barredo, Sylvain De Léséleuc, Vincent Lienhard, Thierry Lahaye, and Antoine Browaeys. An atom-by-atom assembler of defect-free arbitrary two-dimensional atomic arrays. *Science*, 354(6315):1021–1023, 2016.

[43] Daniel Barredo, Vincent Lienhard, Sylvain De Leseleuc, Thierry Lahaye, and Antoine Browaeys. Synthetic three-dimensional atomic structures assembled atom by atom. *Nature*, 561(7721):79, 2018.

[44] Aishwarya Kumar, Tsung-Yao Wu, Felipe Giraldo, and David S Weiss. Sorting ultracold atoms in a three-dimensional optical lattice in a realization of maxwells demon. *Nature*, 561(7721):83, 2018.

[45] Yang Wang, Xianli Zhang, Theodore A Corcovilos, Aishwarya Kumar, and David S Weiss. Coherent addressing of individual neutral atoms in a 3d optical lattice. *Physical review letters*, 115(4):043003, 2015.

[46] Yang Wang, Aishwarya Kumar, Tsung-Yao Wu, and David S Weiss. Single-qubit gates based on targeted phase shifts in a 3d neutral atom array. *Science*, 352(6293):1562–1565, 2016.

[47] D Jaksch, JI Cirac, P Zoller, SL Rolston, R Côté, and MD Lukin. Fast quantum gates for neutral atoms. *Physical Review Letters*, 85(10):2208, 2000.

[48] Klaus Mølmer and Anders Sørensen. Multiparticle entanglement of hot trapped ions. *Physical Review Letters*, 82(9):1835, 1999.

[49] Anders Sørensen and Klaus Mølmer. Quantum computation with ions in thermal motion. *Physical review letters*,

82(9):1971, 1999.

[50] G Pupillo, A Micheli, M Boninsegni, I Lesanovsky, and P Zoller. Strongly correlated gases of rydberg-dressed atoms: quantum and classical dynamics. *Physical review letters*, 104(22):223002, 2010.

[51] Alexandre Dauphin, Markus Mueller, and Miguel-Angel Martin-Delgado. Rydberg-atom quantum simulation and chern-number characterization of a topological mott insulator. *Physical Review A*, 86(5):053618, 2012.

[52] Tyler Keating, Charles H Baldwin, Yuan-Yu Jau, Jongmin Lee, Grant W Biedermann, and Ivan H Deutsch. Arbitrary dicke-state control of symmetric rydberg ensembles. *Physical Review Letters*, 117(21):213601, 2016.

[53] Jongmin Lee, Michael J Martin, Yuan-Yu Jau, Tyler Keating, Ivan H Deutsch, and Grant W Biedermann. Demonstration of the jaynes-cummings ladder with rydberg-dressed atoms. *Physical Review A*, 95(4):041801, 2017.

[54] P Marte, P Zoller, and John L Hall. Coherent atomic mirrors and beam splitters by adiabatic passage in multilevel systems. *Physical Review A*, 44(7):R4118, 1991.

[55] Andrew D Greentree, Jared H Cole, AR Hamilton, and Lloyd CL Hollenberg. Coherent electronic transfer in quantum dot systems using adiabatic passage. *Physical Review B*, 70(23):235317, 2004.

[56] Petr Král, Ioannis Thanopoulos, and Moshe Shapiro. Colloquium: Coherently controlled adiabatic passage. *Reviews of modern physics*, 79(1):53, 2007.

[57] Xi Chen, I Lizuain, A Ruschhaupt, D Guéry-Odelin, and JG Muga. Shortcut to adiabatic passage in two-and three-level atoms. *Physical review letters*, 105(12):123003, 2010.

[58] Tyler Keating, Robert L Cook, Aaron M Hankin, Yuan-Yu Jau, Grant W Biedermann, and Ivan H Deutsch. Robust quantum logic in neutral atoms via adiabatic rydberg dressing. *Physical Review A*, 91(1):012337, 2015.

[59] XL Zhang, L Isenhower, AT Gill, TG Walker, and M Saffman. Deterministic entanglement of two neutral atoms via rydberg blockade. *Physical Review A*, 82(3):030306, 2010.

[60] XL Zhang, AT Gill, L Isenhower, TG Walker, and M Saffman. Fidelity of a rydberg-blockade quantum gate from simulated quantum process tomography. *Physical Review A*, 85(4):042310, 2012.

[61] Sylvain De Léséleuc, Daniel Barredo, Vincent Lienhard, Antoine Browaeys, and Thierry Lahaye. Analysis of imperfections in the coherent optical excitation of single atoms to rydberg states. *Physical Review A*, 97(5):053803, 2018.

[62] J Dalibard and Claude Cohen-Tannoudji. Dressed-atom approach to atomic motion in laser light: the dipole force revisited. *JOSA B*, 2(11):1707–1720, 1985.

[63] Michael Joseph Martin, Grant Biedermann, Yuan-Yu Jau, Jongmin Lee, and Ivan Deutsch. A cphase gate between rydberg-dressed neutral atoms. Technical report, Sandia National Lab.(SNL-NM), Albuquerque, NM (United States), 2018.

[64] Jun Zhang, Jiri Vala, Shankar Sastry, and K Birgitta Whaley. Geometric theory of nonlocal two-qubit operations. *Physical Review A*, 67(4):042313, 2003.

[65] Jun Zhang and K Birgitta Whaley. Generation of quantum logic operations from physical hamiltonians. *Physical Review A*, 71(5):052317, 2005.

[66] Michael H Goerz, Eli J Halperin, Jon M Aytac, Christiane P Koch, and K Birgitta Whaley. Robustness of high-fidelity rydberg gates with single-site addressability. *Physical Review A*, 90(3):032329, 2014.

[67] Line Hjortshøj Pedersen, Niels Martin Møller, and Klaus Mølmer. Fidelity of quantum operations. *Physics Letters A*, 367(1-2):47–51, 2007.

[68] Thad G Walker and Mark Saffman. Entanglement of two atoms using rydberg blockade. In *Advances in Atomic, Molecular, and Optical Physics*, volume 61, pages 81–115. Elsevier, 2012.

[69] II Beterov, II Ryabtsev, DB Tretyakov, and VM Entin. Quasiclassical calculations of blackbody-radiation-induced depopulation rates and effective lifetimes of rydberg  $n$  s,  $n$  p, and  $n$  d alkali-metal atoms with  $n \leq 80$ . *Physical Review A*, 79(5):052504, 2009.

[70] Brian E Mischuck, Seth T Merkel, and Ivan H Deutsch. Control of inhomogeneous atomic ensembles of hyperfine qudits. *Physical Review A*, 85(2):022302, 2012.

[71] Lorenza Viola, Emanuel Knill, and Seth Lloyd. Dynamical decoupling of open quantum systems. *Physical Review Letters*, 82(12):2417, 1999.

[72] Lorenza Viola and Emanuel Knill. Robust dynamical decoupling of quantum systems with bounded controls. *Physical review letters*, 90(3):037901, 2003.